

METHODS OF ABSOLUTE LASER MEASUREMENTS OF GRAVITY-CONSTANT “g”

M.M.S. Gualini*

ABSTRACT

We propose a modified Michelson's interferometer, with some applications in dimensional metrology. The configuration of a Michelson's interferometer, using corner cubes instead of plane mirrors, is further modified in a rectangular parallelogram. A double prism is introduced in one of the branches of the device, in order to obtain a precision of $\lambda/4$ and an accuracy of $\pm\lambda/8$. The same scheme can be applied to develop absolute portable gravimeters. We present an interferometer-version, enabling us to reduce the free-fall dropping height to less than 25 cm, which is that size of any available device of the same class. Another version of the same interferometer enables a theoretical doubling of the dropping-rate and a reduced dropping-length, with an effective improvement of the measurement-precision of g. This solution may lead to a portable absolute dynamic gravimeter. The paper discusses the mathematical model, in terms of transfer-function of “g”, and describes the modified Michelson's interferometer with a ‘futuristic’ solution for a dynamic portable absolute gravimeter.

Keywords: thickness, refraction index, gravity constant “g”, laser absolute portable gravimeter, Michelson's interferometer.

INTRODUCTION

We had proposed the use of a modified Michelson's Interferometer for fast and accurate alignment of U-fold high-power gas laser cavities¹, hinting at a possible further modification. Theoretical work in the latter modification has enabled consideration of some applications in metrology. Infact, the modified Michelson's Interferometer (MMI) presented here can be used to measure rotations with small angles and thickness of transparent components like “optical flats”, with $\pm\lambda/8$ accuracy. It can be used also to test and measure the backlash and motion-linearity of translation stages. But we found a quite interesting application to develop a new absolute laser gravimeter, with improved precision, accuracy and reduced dimensions. Studies²⁻⁷ on previous portable laser

gravimeters have shown that reduction of the free-fall height⁸ and rise and fall⁹ configurations may lead to the design of portable laser gravimeters of improved performances and, above all, enable us to realize also portable absolute dynamic laser gravimeters.

2. GENERAL AND THEORETICAL DISCUSSION

2.1 The two versions of the modified Michelson's interferometer

The two versions of the modified Michelson's interferometer are shown in figures 1 and 2. We will concentrate the discussion on the version with a double prism DPMMI (Double Prism Modified Michelson's Interferometer), owing to its advantages, including a $\lambda/4$ precision and $\pm\lambda/8$ accuracy. Figure 1 shows the original scheme proposed for accurate fast alignment of U-fold laser cavities¹. From this simple design, we derived the DPMMI of figure 2.

A Double Prism is introduced in the scheme of figure 1 and is fixed in its position, once properly aligned. Thus, typical Michelson's fringes can be observed when the displacement, Δp (M_1 and M_2 , part of the same prism, move simultaneously), is equivalent to:

$$\Delta p = (1/2) \cdot (M_p + 1/2) \lambda_0 = (2M_p + 1) \lambda_0 / 4 @ M_p = 0, 1, 2, \dots (1)$$

where λ_0 is the stabilized wavelength of the laser source. Beside the advantages of improved precision and accuracy, the insertion of the double prism enables a direct control of the misalignments. Infact, a double spot detected by the receiver, a CCD camera, instead of the fringes, will be the direct information that the interferometer has lost its alignment. This information can be quantified after proper calibration and the distance between the two spots on the CCD will be proportional to the misalignments. The relative displacement of the two beams on the CCD surface will also enable us to determine the orientation of the misalignments, so that error-compensation can be carried out automatically.

Beside the development of a quite compact, absolute laser gravimeter, the DPMMI has some other

* Pakistan Institute of Lasers and Optics, P.O.Box 1384, Islamabad.

Methods of Absolute Laser Measurements of Gravity-Constant “g”

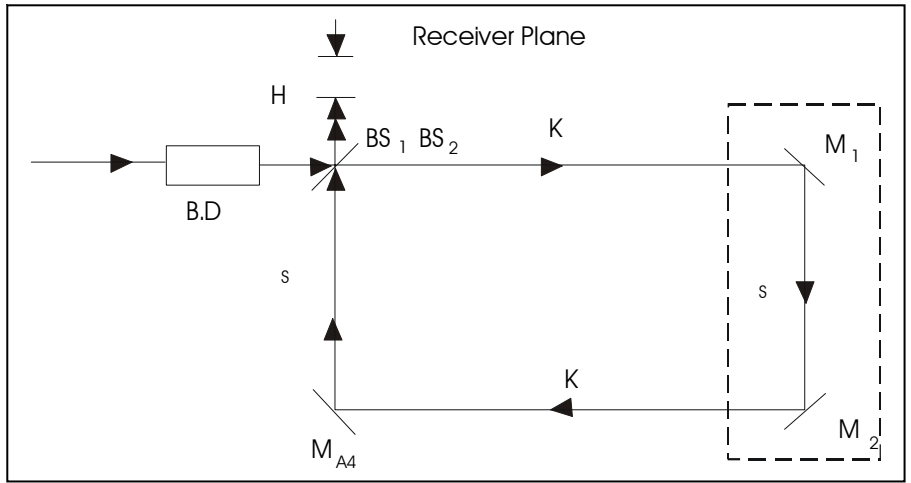


Figure - 1: First version of the modified Michelson's interferometer¹.

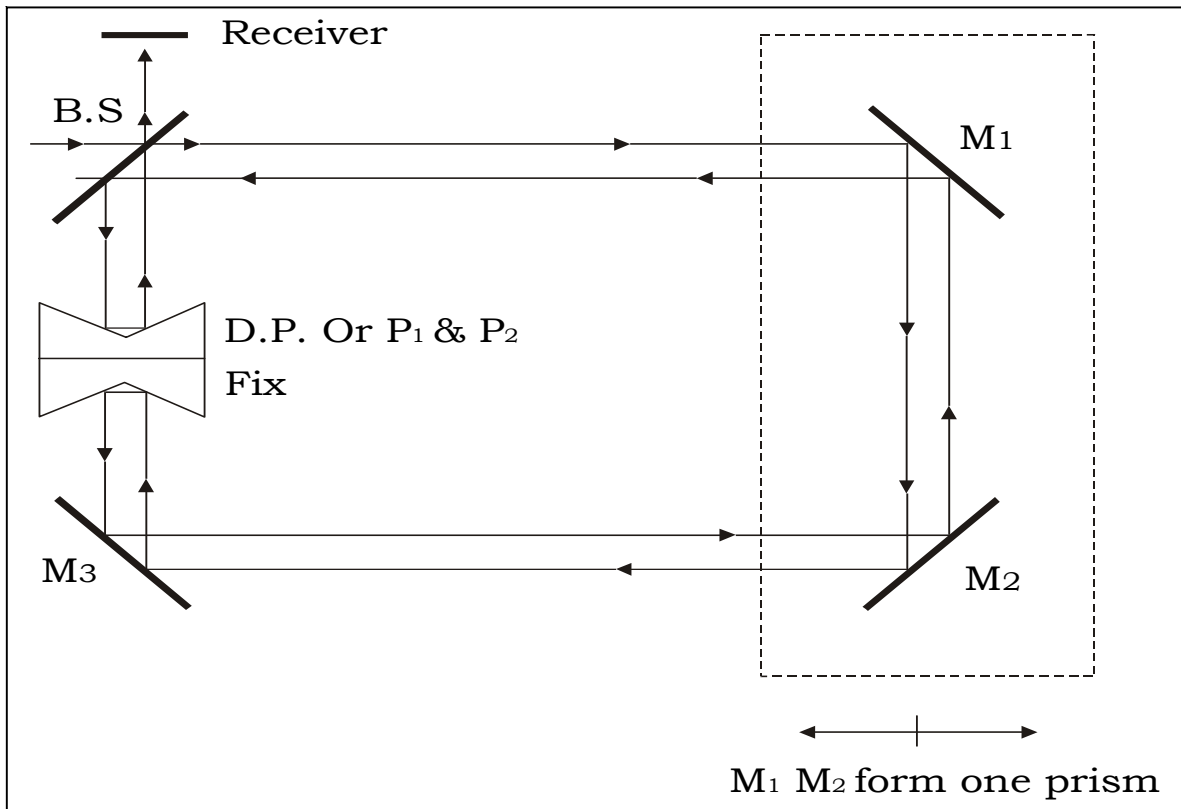


Figure - 2: Final version of the modified Michelson's interferometer¹.

applications in Metrology, which are briefly discussed in the following section.

2.2 Some applications in Metrology

With reference to figure 2, the DPMMI can be used to test and characterize translation-stages, once M_1 and M_2 , part of the same prism, are installed on the moving part of a precision sliding ruler, or a translation stage. Positional accuracy and repeatability can be monitored and measured directly; eventual backlash and tilts can be indicated by the missed overlapping of the two interfering beams, as already discussed above.

The DPMMI can also be used for precision measurement of small rotary angles, or the measurement of the thickness or refractive index of transparent flat components, as is visible in figure 3. The transparent object of thickness t and refractive index n_β will introduce a beam path-difference Δp , so that the number of fringes M_p may be counted. From figure 3 it can be easily derived that $\Delta p = t/\cos\beta$, which can be compared with the measured $\Delta p = (2M_p + 1)\lambda_0/4$ @ ($M_p = \text{integer}$), so that we can write the identity expressed by equation (2):

$$t/\cos\beta = (2M_p + 1) \lambda_0/4 @ M_p = \text{integer read out from counter} \quad (2)$$

Equation (2) can be used to determine, alternatively, thickness or refraction index of the transparent object under test, when the other variable is known. Assuming that n_α , the refraction index in vacuum, is equal to 1, the Snell's law, $n_\alpha/n_\beta = \sin\alpha/\sin\beta$, becomes $n_\beta = 1/\sin\beta$, since $\alpha = 90^\circ$. A method to measure contemporarily the thickness of the transparent object and its refractive index, taking advantage of the interferometer accuracy. This is possible when we install the transparent object on a rotary stage and take two measurements, one with $\alpha = 90^\circ$ and the other with $\alpha = 85^\circ$ that corresponds to a rotation of the transparent object by $\delta = 5^\circ$, for example. By the square triangle property and the Snell's law, we can write a set of two equations with two variables, t and β , as follows:

$$t/\cos\beta = (2M_1 + 1) \lambda_0/4 \equiv a, @ M_1 = \text{integer from counter read out} \quad (3)$$

$$t/[\cos(90^\circ - \delta - \beta)] = (2M_2 + 1) \lambda_0/4 \equiv b, @ M_2 = \text{integer from counter read out} \quad (4)$$

where "a" and "b" are known from the measurement of

the fringes, $(2M_1 + 1) \lambda_0/4 \equiv a$ and $(2M_2 + 1) \lambda_0/4 \equiv b$, respectively. Assuming $\delta = 5^\circ$ and developing $\cos(90^\circ - \delta - \beta) \equiv \cos(85^\circ - \beta)$ in $(\cos 85^\circ \sin\beta + \cos\beta \sin 85^\circ) = k_1 \sin\beta + k_2 \cos\beta$, where $k_1 = 0.087155\dots$ and $k_2 = 0.996194\dots$. After obvious passages, the solutions of the two variables set of equations (3) and (4) is represented by:

$$\beta = \arctan[(1/k_1)(b/a - k_2)]; t = b \cdot \cos\beta; n_\beta = 1/\sin\beta \quad (5)$$

PC software may solve automatically for the values expressed by equations (5), once data (M_1, M_2, δ) are properly entered.

3. THE PROPOSED PORTABLE ABSOLUTE LASER GRAVIMETER

There are many types of gravimeters, each of them based on a different physical principle. Main distinction is between absolute and relative gravimeters. The first type calculate gravity from data directly measured with primary standard instruments, while the latter rely on indirect relations with primary standards. Majority of portable gravimeters adopt the so-called "free falling" method. An optical prism, the mass, is dropped inside the chamber, defined as "dropping-chamber". The descent of the free-falling object is monitored very accurately, using a Michelson interferometer with prismatic mirrors. Therefore, the measure of the free-falling path is reduced to a fringe-count, using an electronic digital counter. The total fringe count, N , is then multiplied by the interferometer fringe order, $\lambda_{\text{HeNe}}/2$ in the case of HeNe laser source in a Michelson type, so that $H \equiv N \times \lambda_{\text{HeNe}}/2$. The free-falling time is measured by an atomic clock, generally a portable rubidium device. The HeNe laser emission-frequency is locked on a stable and repeatable atomic transition. Laboratory-made devices of this type have long-term stability better than $\Delta\lambda/\lambda_0 = 10^{-9}$, λ_0 being the locking wavelength. Since the definition of the meter, as absolute length-standard, is a multiple of this λ_0 , therefore the value $H \equiv N \cdot \lambda_{\text{HeNe}}/2$ represents an absolute measure. An atomic rubidium clock registers the free-fall time between two reference points, thus allowing an absolute time measure. Consequently the value of g calculated in the case of the free-fall gravimeter² and obtained from the following equation is an absolute value:

$$g = 8 \cdot H / (T_1^2 - T_h^2) \quad (6)$$

Methods of Absolute Laser Measurements of Gravity-Constant “g”

Where H is the free-fall length, T_1 and T_h are the start and stop times, respectively, corresponding to the same free-fall length. General scheme of this gravimeter is shown in figure 4, from reference 6. A motor drives a cart that falls with the corner-cube - prism. The laser beam back-reflected by the reference corner cube prism combines with the beam back-reflected from the free-falling corner-cube-prism on the surface of the photo detector, generating classic Michelson fringe patterns. An oscilloscope monitors and records the interference fringes, while, in parallel, a counter counts them. Reference photo-detectors automatically start and stop fringes-count and time-measure.

In order to appreciate the improvements of the proposed solution with respect to the current available portable absolute gravimeters, we briefly recall here below the state-of-the-art of this class of instruments.

3.1 First generation free-fall absolute gravimeters

Drawbacks of the first-generation free-fall absolute gravimeters are their size and weight. Despite the claimed portability, the devices were quite heavy and cumbersome, requiring separate vacuum-pump and a rack holding all the basic instruments and the service electronics. Also, the laser would have been installed separately, eventually complicating alignment procedures. For example, the first prototype of the device described in reference² was almost 1.5 m tall and ~300 kg total weight. The commercially available FG5-L⁸ has a weight of 57 kg and is 0.75 m tall. But the absolute gravimeter recently introduced and described in reference⁴ is basically one fifth of the size of the FG5-L, which makes it a possible candidate for absolute dynamic measurements. Reduction in size of lasers, PC's, electronic boards and vacuum pumps will be the determinant to further reduce the size of future devices of the same type.

Easy transportability is not the only reason behind the continuous trend to reduce the size of absolute gravimeters. In fact, as pointed out by Marson and Faller⁹, the slow acquisition-time was assumed as being the main limitation of the R&F free-fall absolute gravimeters. Quite obviously, longer is the ballistic trajectory, H , the longer is the total time of measurement, including the time to invert the path, as is quite evident from figure 5, showing the

characteristic transfer-function of a rise-and-fall device². Shorter acquisition-time means higher precision. For example, the latest device described in reference⁴ has a throw-rate of 100 cycles/minute and a best-case single-throw precision of $\pm 4.0 \mu\text{Gal}$ (1 Gal = 1 Galileo = 1 cm/sec² - in these units $g = 980 \text{ Gal}$). The precision of the early prototype of reference 2 was $\pm 20.0 \mu\text{Gal}$ and its throw-rate in the range of 2–5 per minute, which was preventing a full field operation, due to the effects of perturbations like wind and temperature changes. The total free-fall time per minute of observation has increased almost one order of magnitude, compared to other previous devices⁴.

Therefore, size-reduction is extremely important to improve the performances of absolute free-fall gravimeters, leading towards full field dynamic absolute, g , and measurements. Figure 6 shows the surface graphic of the total height, $H = 1.22625 (T_1^2 - T_h^2)$, in case of R&F-systems. Figure 6 shows that, in order to have measurement periods of 200 ms, the chamber height has to be approximately 50 cm. Similarly, for the single drop in free-fall, the authors of reference 4 report a limit of 20 cm for the drop height, for the same measurement period. Obviously it is a matter of trade-off between period of measurement and height of drop. It is worth noticing that an height of 35 cm is reasonably comparable to a portable dynamic gravimeter, but in the case of spring-type meters, the typical filter duration is 120 s or more, while free-fall devices show measurement-periods shorter than 200 ms.

The advantage of short drop-heights is double, gain in the form of size-reduction and increasing the measurement-time or duty cycle⁹. In fact, the repetition-rate directly influences the measurement-precision, this precision is usually given in $\mu\text{Gal}/\sqrt{\text{Hz}}$. From equation (6), figure 4 and 5, it is quite evident that the shorter the stop time, T_h , the higher will be the repetition-rate and, consequently the precision in $\mu\text{Gal}/\sqrt{\text{Hz}}$. A value reported from reference⁴ is of $3 \mu\text{Gal}/\sqrt{\text{Hz}}$.

3.2 The Drop method versus Rise and Fall (R&F)

Practical realization of an absolute gravimeter is not a simple task, especially from a mechanical point of view. Beside the necessary design that may grant

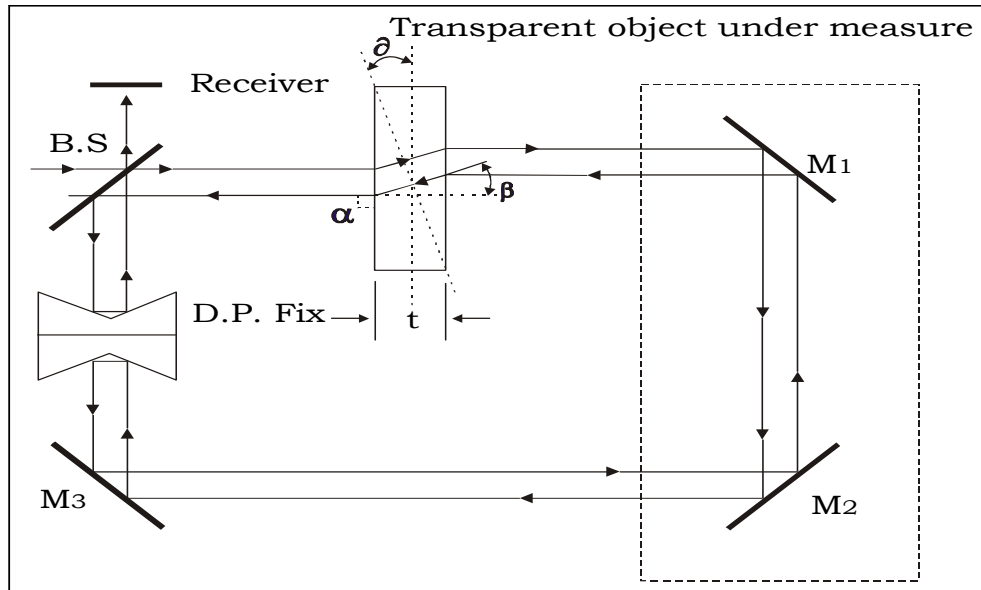


Figure 3: DPMMI setup to measure thickness and refraction index of transparent objects.

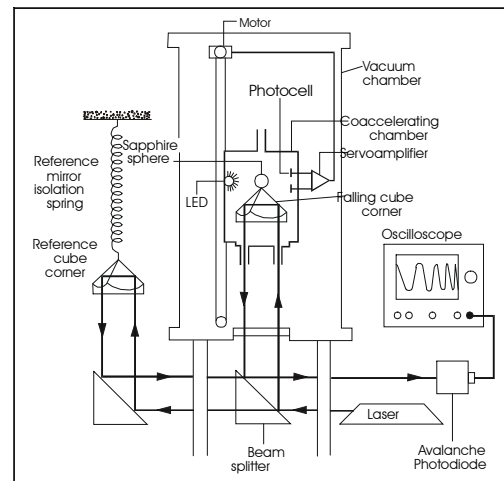


Figure 4: Diagram of the free-fall apparatus from reference⁶.

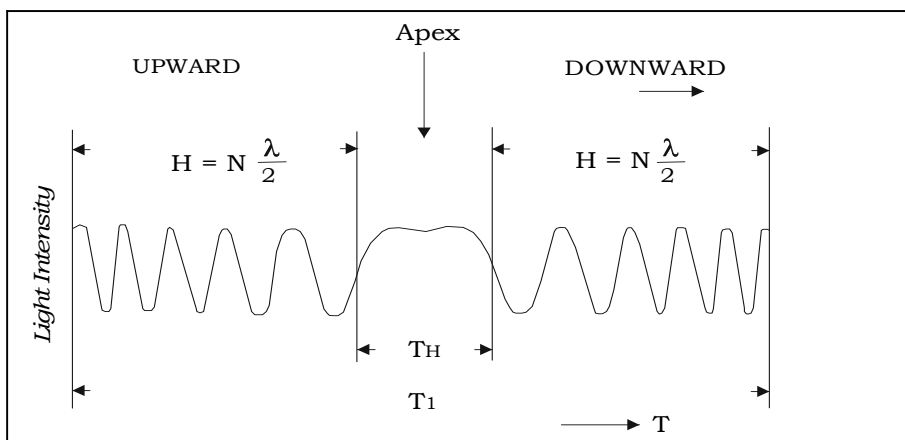


Figure 5: Characteristic transfer function of a R&F absolute gravimeter²

Methods of Absolute Laser Measurements of Gravity-Constant “g”

reasonable insulation from various source of vibrations, the key point is the mechanism to launch or drop the mass, i.e. an optical prism protected by a cart. The cart has the function to offer the necessary friction to the retaining system used to launch or drop the prism, without disturbing the optical alignment of the latter.

But it offers also the possibility to reduce the effects of the buoyant residual force, since the normal operating vacuum condition is 10^{-6} Torr. Authors² have reported correction-factor of buoyant force in the order of $5 \mu\text{Gal}/\text{Pa}$, partially compensated by the correction required for the wavelength-reduction in the operating vacuum conditions, $3 \mu\text{Gal}/\text{Pa}$. Thus the measure requires a total correction in the range of $\sim 2 \mu\text{Gal}/\text{Pa}$. Moreover, the cart protects also against residual influences of the magnetic fields and other sources of noise for the measurements. The above mechanical problems are more complicated in case of R&F respect drop-devices. In fact the majority of absolute free-fall gravimeters are designed in drop-configuration to simplify the launching mechanics. But also to take advantage of the minimal errors produced by a practically zero value of the vertical component of its speed, which would influence the measure, but not the alignment of the interferometer, owing to the propriety of an optical prism indicated in figure 7.

R&F absolute gravimeters offer better performances, although these are more complicated to be realized from a mechanical point of view. In fact, R&F devices have a symmetric behavior, as visible in their characteristic curve reported in figure 5. The symmetric behavior has the benefit of compensating many errors⁹ owing to opposite actions from upward (rise) and downward (fall) motion. Resistance of the residual air in the dropping chamber, magnetic fields and position errors will be also eliminated by the double directionality of the design.

The benefits of shorter dropping chambers and consequent increase of the measurement-time have been already underlined above. A drop only gravimeter, like the FG5-L, operates at a best-case rate of one drop every 2 s with a best-case duty cycle of $0.2\text{s}/2\text{s}$ or one tenth.

4. DESCRIPTION OF THE PROPOSED NEW GRAVIMETER

We propose in the following a possible improvement to the latest generation of portable absolute gravimeters, adopting a R&F configuration, reducing consequently the size while contemporarily increasing the measurement-period. We have also devised some extra features, in the attempt to improve the single-drop figure, trying to attain, at least theoretically, a global value better than $\pm 0.5 \mu\text{Gal}/\text{drop}$.

The device here proposed has essentially the following innovations:

1. Higher optical fringes-resolution, owing to a peculiar modification of the classic Michelson's Interferometer configuration
2. New design-concepts, minimizing the dropping height
3. New design concepts, reducing the “stop time” and increasing the “throw-rate”.

4.1 Higher optical fringes resolution of the modified classic Michelson's Interferometer

The scheme of figure 2 is proposed, in order to develop a third-generation of laser gravimeters. The advantage of this configuration is that the displacement H_N corresponds to:

$$H_N = (1/2) \cdot (M + 1/2) \lambda_0 = (2M + 1) \lambda_0 / 4 \quad (7)$$

Where M is an integer (= 0, 1, 2, 3...). The fringe-order in this case is $\lambda_0/4$, and its accuracy $\pm \lambda_0/8$. This represents an effective advantage because, with the same number of counted fringes, i.e. $N \equiv (2M + 1)$, we find that $H_N = H/2$. In other words we have reduced the drop height of a Michelson's interferometer in half, without compromising in measurement-precision. Basically, if we have a drop-height of 35 cm with a R&F system, using a conventional Michelson's interferometer, then with the proposed solution we have a theoretical 17.5 cm dropping path with a considerable reduction of the related chamber. It is possible to consider feasible dropping-heights of 10 to 15 cm, thus matching with the size of transportable dynamic gravimeters. The advantages of shorter drop-height will be also beneficial to the measurement period rate and the instrument-precision, expressed in $\mu\text{Gal}/\sqrt{\text{Hz}}$, as discussed above. Thus, the first claim that we propose a more precise and accurate gravimeter is satisfied, since in the DPMMI

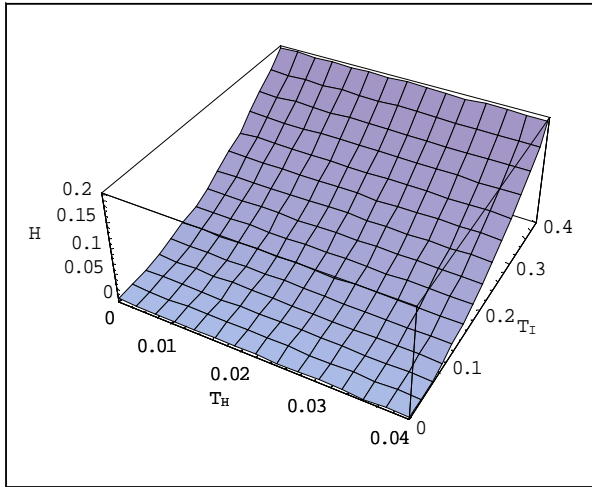


Figure 6: Surface graphic of H , drop height, in function of the total, T_T , and stop, T_H , times.

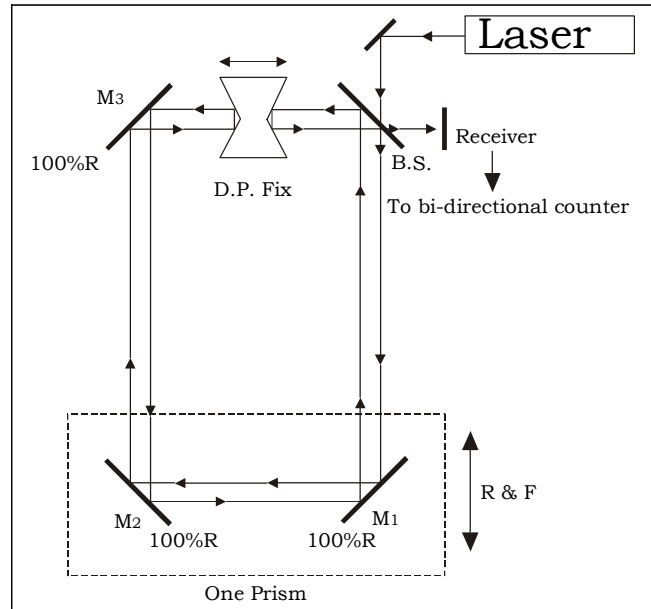


Figure 8: First gravimeter version based on the DPMMI.

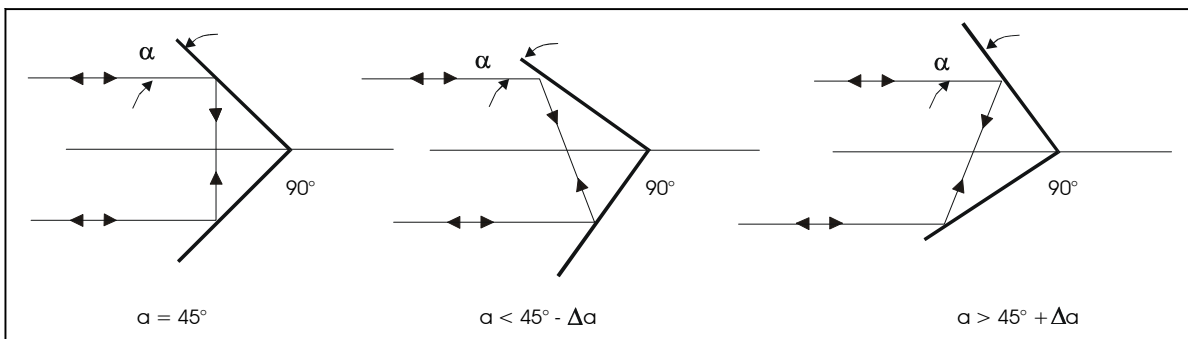


Figure 7: The propriety of the optical prism reduces misalignment errors.

Methods of Absolute Laser Measurements of Gravity-Constant “g”

case, the precision is $\lambda_0/4$, and accuracy is $\pm \lambda_0/8$.

4.2 New design concepts minimizing the dropping height

The adoption of the DPMMI introduces the possibility to reduce the effective height of the dropping chamber by half of the current devices, as demonstrated above with equation (7). The intrinsic accuracy of fringe-count of the proposed interferometer improves (by 1/8 factor) the figure of a classic Michelson's interferometer, thus giving an expectancy of $\pm 0.5 \mu\text{Gal/drop}$ accuracy and precision of $\pm 1.0 \mu\text{Gal/drop}$.

We notice that the proposed DPMMI suggests the adoption of two interesting and perhaps quite “innovative” solutions, without compromising the newly introduced benefits. The ideas are shown in figure 8 and figure 9. Figure 8 shows a gravimeter-scheme close to the classic concept discussed above. The free-falling prism is represented by M_1 and M_2 , which must be regarded as a single prism. This improvement can be adopted directly on the present gravimeters by simply introducing conveniently the double prism in the optical path in a kind of a retrofitting. The direct benefit expected in this case is the shortening by half of the dropping height and consequently an increase of the precision by the increase of the dropping-rate and the intrinsic higher precision of the DPMMI.

But the DPMMI offers a more interesting and alternative scheme to that of figure 8, which is shown in figure 9. In this case, the double prism is in reality formed by two separate prisms, P_1 and P_2 . Using a dropping chamber shorter than any other dropping chambers, almost half of their falling height. Thus we can imagine developing a double launching system that throws alternatively P_1 and P_2 , so that we obtain two benefits. The first benefit is that the dropping chamber is shorter and thus the advantages of the scheme described in figure 8 are preserved. But in this case, we can imagine an automatic system that controls the alternate launch and drop of P_1 and P_2 in order to reduce the duty-cycle between two subsequent drops almost to zero. Thus, in the case of the scheme described in figure 9, we enjoy the reduction by half of the dropping height and almost a *four times* increase of the dropping-rate. Infact we consider (a) two times, due to reduction by half of the

dropping height and (b) two times, due to reduction to almost zero of the dropping rate duty-cycle by launching alternatively P_1 and P_2 .

We notice that adopting the two-prisms solution gives, in itself, a kind of double-directionality to the system, so that we can consider rotating the branch of the interferometer containing the two prisms, while the other part remains fixed. This is possible without introducing sensible misalignments in the interferometer, due to the properties of the optical prisms already underlined in figure 7. In this way, the dropping chamber can be turned like a sand-clock. Quite interestingly, we may imagine to introduce a double mechanism so that inside the dropping chamber will be a double rise-and-fall launching system, while the sand-clock type of operation will ensure a further alternate drop regime.

In this way we may conceive an automatic control-system that alternates cycles of single-drop regime with those of rise-and-fall launches, synchronized with the continuous rotation of the dropping chamber. The advantage is that, by comparison, one may correct the systematic errors introduced by the launch-speed components that may interfere with the measure, as above discussed. It is quite possible to develop dedicated software that controls all the functions of driving the rotations of the dropping chamber, the alternate dropping regime of P_1 and P_2 and handles, in parallel, the data acquisition. The idea for this is shown in figure 10.

The transfer function of the conventional R&F laser portable gravimeter, based on a classic Michelson's Interferometer, has the behavior already shown in figure 5. In fact, the transfer function in this case is expressed by equation (8):

$$I = (2A^2/Z)\text{Cos}^2[(k/2) \cdot \Delta z] = (2A^2/Z)\text{Cos}^2[(\pi/\lambda)(g/8) \cdot t^2] \quad (8)$$

where A is the laser-source irradiance (W/m^2), Z is the intrinsic impedance in free space ($Z = 377 \Omega/n$, n is the refractive index of the medium, in case of vacuum $n = 1$), k is the amplitude of the propagation vector, $k = 2\pi/\lambda$. Equation (8) is the result of the application of the theory of propagation of electromagnetic waves interference, expressing the laser-light waves from the Maxwell equations in polar coordinates for the center of the interferometric pattern,

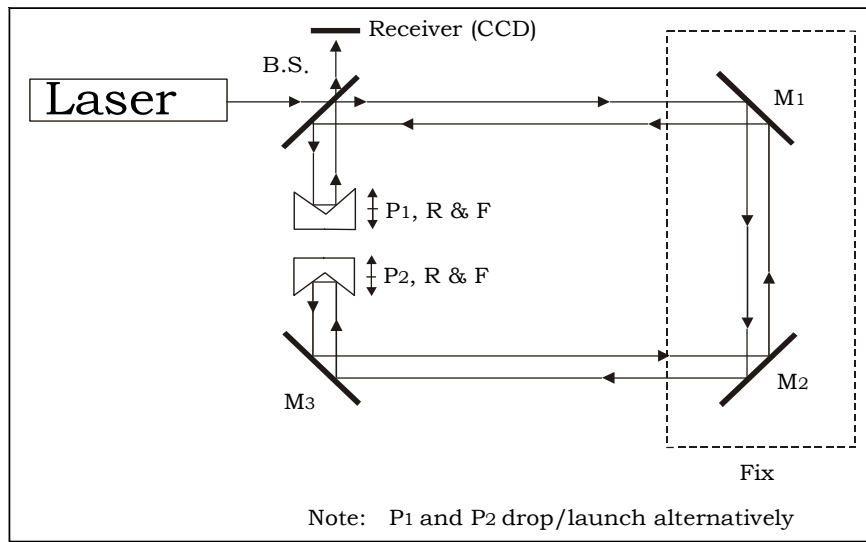


Figure 9: Second gravimeter version based on the DPMI.

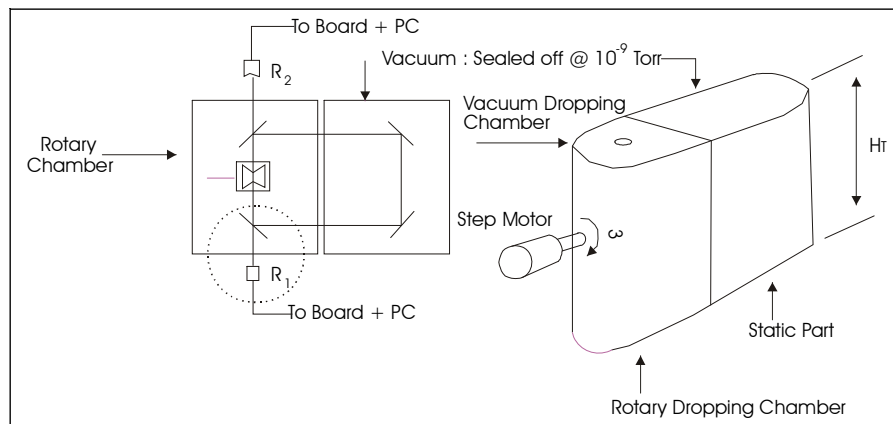


Figure - 10: "Futuristic" concept. For simplicity, beam paths are single lines and prisms shown not separated, as they must be to obtain optical fringes.

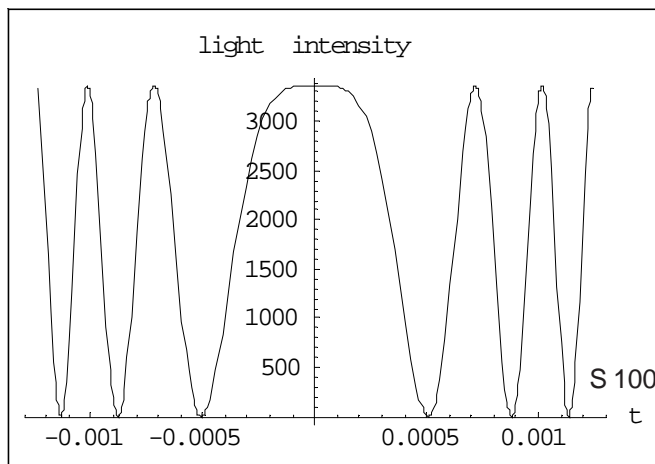


Figure - 11: Transfer function of an R&F currently available laser portable gravimeter.

Methods of Absolute Laser Measurements of Gravity-Constant “g”

$r = 0$. More particularly, equation (8) is obtained from the standard relation of the light-intensity of a classic Michelson’s interferometer, available from literature¹⁰, which is an acceptable approximation. In details, we have imposed in equation (8) that the beam path-difference, Δz , that generates the phase-shift to produce the fringes, is coincident with the dropping height, $H \equiv \Delta z$, and solving equation (1) in H , $H = g \times (t^2/8)$, assuming for simplicity $t^2 = T_1^2 - T_h^2$, which means not considering the inversion motion time, $T_h^2 = 0$, basically not of interest in a theoretical approach. After substitutions and manipulations, equation (8) is obtained. Equation (8) can be adopted to simulate the transfer-function of real cases, by simply substituting experimental data. Assuming an R&F device operating with a conventional Michelson’s interferometer, we can substitute real parameters and values in equation (8) and then compare it with the transfer-function of the devices proposed in figure 8 and 9. For example, assuming working with a frequency-stabilized HeNe laser of 5 mW output power, with a 632 nm vacuum wavelength and a beam diameter at the source of 2 mm, a dropping height of 0.30 m, we find a transfer-function expressed by equation (9), whose behavior is reproduced here in figure 11 below.

$$I = 3362.86445 \cdot \text{Cos}^2[(3.14 \cdot 9.8)/(8.0 \cdot 632.0 \cdot 10^{-9})(t^2)] \quad (9)$$

Conversely, the following equation (10) shows the transfer function for an R&F laser portable gravimeter, adopting the proposed modified Michelson’s interferometer with the same parameters of equation (9). The behavior of equation (10) is visualized in figure 12.

$$I = 3362.86445 \cdot \text{Cos}^2[2 \cdot (3.14 \cdot 9.8)/(8.0 \cdot 632.0 \cdot 10^{-9})(t^2)] \quad (10)$$

Comparison between figures 11 and 12 gives a clear idea of the advantages of adopting the proposed modified Michelson’s interferometer in one of the two versions proposed above. In fact, for the same dropping height, the number of counted fringes is double for the proposed solution. This is clear evidence that the proposed configuration enables shortening the dropping-height by half and, consequently, enables increasing the throw rate. At half dropping-height, the transfer-function given by equation (10) overlaps the one represented in figure 10, which encourages us to assume, at least theoretically, that the class of

precision of the instrument will be at least the same of any available R&F devices operating with a conventional Michelson’s interferometer, but with higher accuracy.

Differentiating equation (10) as a function of the variable time, t , we obtain the theoretical intensity fluctuations in function of the time:

$$dI/dT = -1.6373710^{11} t \text{Cos} 1.2172510^7 t^2 \text{Sin} 1.2172510^7 t^2$$

We have drawn the corresponding diagram in figure 13. The diagram shows clearly that the shorter the R&F time-duration, the intensity fluctuations, which may influence the readings of the instrument, will not influence the measure.

Similarly, in the case of a conventional R&F gravimeter, the behavior of the intensity-fluctuations will be similar, but the system shows a better tolerance to relatively longer R&F times, as visible in figure 14.

4.3 New design-concepts, reducing the stop-time and increasing the “throw rate”

The systems described in figures 8 and 9 may effectively help in increasing the “throw rate” by a drastic reduction of the measurement-period, provided a suitable process-control is introduced. The process-control will also enable the fully automatic measurement procedure. In this case, the device appears to be, at least theoretically, an interesting candidate to become an effective *transportable* absolute dynamic gravimeter.

5. CONCLUSIONS

We have introduced a modification to the classic Michelson’s interferometer, already described in previous works, by introducing a double prism. This second modified interferometer enables us to reduce by half the size of the dropping chamber, without compromising on the final precision and accuracy of the instrument. We have proposed two schemes that can give benefit of the shorter dropping chamber. The first scheme enables also increasing the drop-rate to

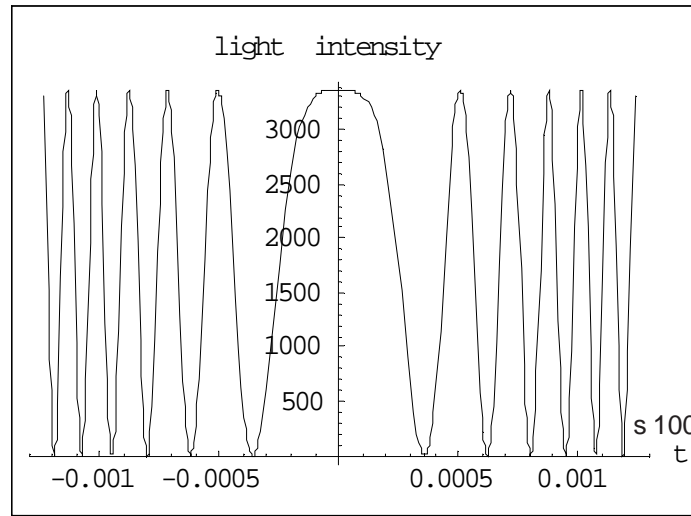


Figure - 12: Transfer function of the newly proposed R&F laser portable gravimeter.

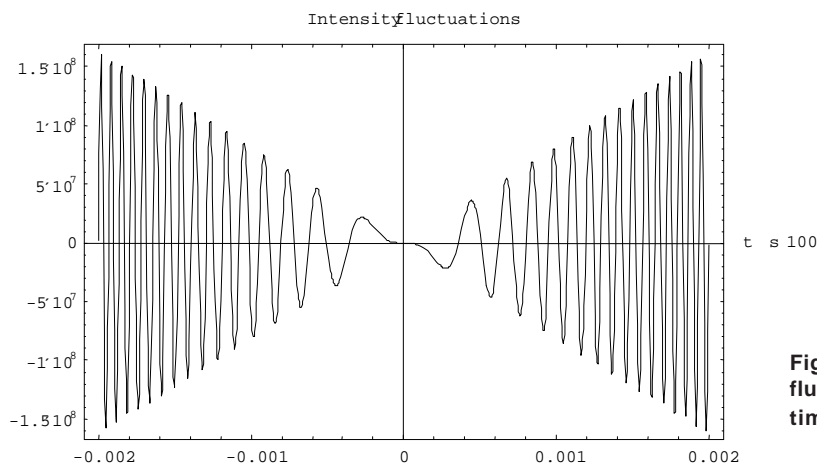


Figure - 13: theoretical intensity fluctuations in function of the R&F time for the proposed gravimeter.

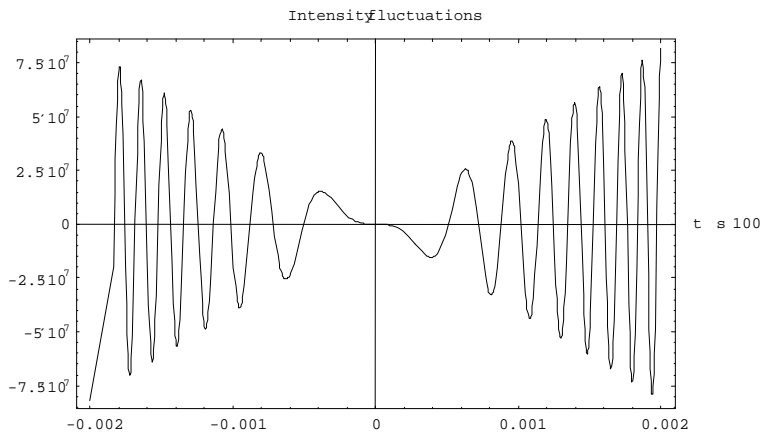


Figure - 14: theoretical intensity fluctuations in function of the R&F time for a conventional portable laser gravimeter.

Methods of Absolute Laser Measurements of Gravity-Constant “g”

further improve the final precision of the instrument on the averaged values.

The second scheme, with two prisms launched alternatively, enables us to increase the launching rate theoretically by four times. In order to get benefit from the advantages of the R&F and drop configuration and the alternate launch of the two prisms, combined together, we have proposed a “futuristic” scheme where rise-and-fall launches are alternate to simple drops, thus enabling mutual compensation of the systematic errors typical to each of the two configurations.

It is finally expected that improved frequency-stability schemes of laser sources and corresponding size-reduction will enable one to build very compact and transportable absolute gravimeters candidate, to be used in dynamic measurement conditions.

ACKNOWLEDGEMENTS

The author is particularly thankful to the Chairman of Pakistan Institute of Lasers and Optics (PILO) for his co-operation to allow the presentation of this work. The author feels deeply indebted to Prof. Dr. Ing. Sergio Sartori (formerly director of the Istituto di Metrologia Colonnetti of Turin, Italy) for providing useful suggestions and encouraging this publication. Also, particular thanks to the never-failing support of my family.

REFERENCES

1. M. M. S. Gualini, “Two Beams Laser Ranging, Leveling and Aligning System”, ICALEO’98 Proceedings Volume **85a**, Orlando (November 16-19, 1998)
2. G. Cerutti, L. Cannizzo, A. Sakuma, J. Hostache, “A transportable apparatus for absolute gravity measurement”, *VDI Berichte Nr 212*, 1974
3. F. Alasia, L. Cannizzo, G. Cerutti, I. Marson, “Absolute gravity acceleration measurements: Experiences with a transportable gravimeter”, *Metrologia* **18**(4), 221-229, 1982
4. J.M Brown, T. M. Niebauer, B. Richter, F.J. Klopping, J.G. Valentine and W.K. Buxton, “Miniaturized gravimeter may greatly improve measurements”, from http://www.agu.org/eos_elec/99144e.html
5. J. M. Brown, T.M. Niebauer, F.J. Klopping, A. T. Herring, “A new differential fiber optic gradiometer for 4-D absolute differential gravity”, *Geophysical Research Letters*, Vol.**27**, No. 1, pages 33 – 36, January 1, 2000. Also see J. Wallace, “INTERFEROMETRY: Fiber coupling improves gravimeters”. *Laser Focus World*, **36**(3), March 2000
6. J.E. Faller, I. Marson, “Ballistic methods of measuring g: the direct free fall and symmetrical rise and fall methods compared”, *Metrologia* (1), **25**, 49-55, 1988. Also in Resnick, Haliday, Krane, *Physics*, Volume 1, J. Wiley & Sons, Inc. 1992, 4th Edition, page 27
7. M. M. Gualini, “Portable Laser Gravimeter”, Proceedings (to be published) 2nd International Symposium on Mechanical Vibrations, Islamabad (September 2000)
8. Web page of Micro-g Solutions, Inc. <http://www.microgsolutions.com/> and particularly the site dedicated to the FG5-L, <http://www.microgsolutions.com/fg5l.htm>
9. I. Marson, J.E. Faller, “The acceleration of gravity: Its measurement and importance”, *J.Phys. E. Sci. Instrum.*, **19**, pages 22-32, 1986
10. J.T. Luxon, D.E. Parker, *Industrial Laser Applications*, Prentice-Hall (1984)